ESMO GOOD SCIENCE BETTER MEDICINE BEST PRACTICE

IOTECH IMMUNO-ONCOLOGY AND TECHNOLOGY

ORIGINAL ARTICLE

Characterization and translational development of IOA-289, a novel autotaxin inhibitor for the treatment of solid tumors

M. A. Deken[1*], K. Niewola-Staszkowska[2], O. Peyruchaud[3], N. Mikulčić[4], M. Antolić[4], P. Shah[5], A. Cheasty[5], A. Tagliavini[6], A. Nizzardo[6], M. Pergher[6], L. Ziviani[7], S. Milleri[7], C. Pickering[2], M. Lahn[2], L. van der Veen[1], G. Di Conza[2] & Z. Johnson[2†]

[1]iOnctura, Amsterdam, the Netherlands; [2]iOnctura, Geneva, Switzerland; [3]INSERM, UMR 1033, Faculté de Médecine Lyon Est, Université Claude Bernard Lyon 1, Lyon, France; [4]Selvita, Zagreb, Croatia; [5]Cancer Research Horizons, Therapeutic Discovery Laboratories, Cambridge, UK; [6]Aptuit (Evotec), Verona; [7]Centro Ricerche Cliniche di Verona srl, Verona, Italy

Available online 8 April 2023

Background: Autotaxin-lysophosphatidic acid (ATX-LPA) signaling has a predominant role in immunological and fibrotic processes, including cancer. Several ATX inhibitors and LPA receptor antagonists have been clinically evaluated, but none in patients with solid tumors. Many cancers are burdened with a high degree of fibrosis and an immune desert phenotype (so-called 'cold' tumors). In these cold tumors, the fibrotic stroma provides an intrinsic cancer-supporting mechanism. Furthermore, the stroma prevents penetration and limits the effectiveness of existing therapies. IOA-289 is a novel ATX inhibitor with a unique chemical structure, excellent potency and an attractive safety profile.

Materials and methods: *In vitro* and *in vivo* pharmacology studies have been carried out to elucidate the pharmaceutical properties and mechanism of action of IOA-289. A phase I clinical study in healthy volunteers was carried out to determine the pharmacokinetics and pharmacodynamics of IOA-289 following a single oral dose.

Results: *In vitro* and *in vivo* studies showed that IOA-289 is a potent inhibitor of ATX and, as a monotherapy, is able to slow progression of lung fibrosis and tumor growth in mouse models. In a clinical study, IOA-289 showed a dose-dependent increase in plasma exposure levels and a corresponding decrease in circulating LPA.

Conclusions: Our data show that IOA-289 is a novel ATX inhibitor with a unique chemical structure, excellent potency and an attractive safety profile. Our data support the further development of IOA-289 as a novel therapeutic approach for the treatment of cancer, particularly those with a high fibrotic and immunologically cold phenotype.

Key words: autotaxin (ATX), lysophosphatidic acid (LPA), inhibitor, immuno-oncology, stroma

INTRODUCTION

Autotaxin (ATX) is a secreted glycoprotein that was originally identified as a tumor cell autocrine motility factor secreted by melanoma cells and later shown to be responsible for the lysophospholipase D (lysoPLD) activity in human serum, hydrolyzing lysophosphatidylcholine (LPC) to lysophosphatidic acid (LPA).[1,2] Present in most biological fluids, LPA signaling has been implicated in a wide range of biological processes and can be found at elevated levels in many diseases including cancer and fibrosis.[3] LPA is rapidly degraded by lipid phosphate phosphatases (LPPs) and has a limited half-life of ∼1 min.[4] Downstream effects of LPA are therefore regulated by the balance of LPA formation by ATX versus LPA degradation by LPPs.[5]

It is well established that through the generation of LPA, ATX is implicated in several cancers as a direct driver of tumor growth and, in particular, tumor spread.[6] The expression level of the gene encoding for ATX, *ENPP2*, and the ATX protein itself are often elevated in many cancer types, including pancreatic cancer, glioblastoma, lung and breast cancer, renal cell carcinoma and lymphoma. This overexpression of ATX leads to high levels of LPA which cannot be balanced by LPP-mediated degradation. Furthermore, many cancers are characterized by extracellular matrix deposition that drives a fibrotic phenotype, and fibrosis is recognized as one of the hallmarks of cancer. Up to 40% of cancers have been described as having a fibrotic phenotype across TCGA tumors and this phenotype has been linked to a poor response to immunotherapy.[7] As the ATX-LPA pathway is a key driver of fibrosis, it is therefore expected that this pathway will also play a role in the

*Correspondence to: Dr Marcel A. Deken, iOnctura BV, Gustav Mahlerplein 102, 1082 MA Amsterdam, the Netherlands. Tel: +31 641 28 75 56
E-mails: m.deken@ionctura.com or info@ionctura.com (M. A. Deken).

†Present address: Affivant, Basel, Switzerland.

development of tumor fibrosis. Indeed, it has been shown that in pancreatic cancer, tissue-resident pancreatic stellate cells transdifferentiate into activated cancer-associated fibroblasts. In turn, these fibroblasts secrete high levels of LPC that is converted to LPA by ATX secreted by pancreatic ductal adenocarcinoma (PDAC) cells, promoting cancer cell proliferation and migration.[8] The ATX-LPA pathway has also been implicated in the inflammatory crosstalk between cancer cells and stromal cells in breast cancer where ATX is produced by adipose tissue and blocking ATX with the small molecule inhibitor ONO-8430506 has been shown to delay breast tumor growth and lung metastases in a mouse model.[9] Turning to effects on the immune cells in the tumor microenvironment, LPA has been shown to inhibit T-cell activation *in vitro*.[10] In addition, LPA is chemorepulsive to the migration of T cells and single-cell data from melanoma tumors are consistent with intratumoral ATX acting as a T cell repellent, highlighting the potential value of ATX inhibitors in cancer immunotherapy, particularly in combination with checkpoint therapies.[11]

To date, no therapeutic approaches targeting the ATX-LPA pathway have been tested in clinical trials for cancer, whereas the role of the ATX-LPA signaling pathway in fibrotic diseases has been studied in many indications, including idiopathic pulmonary fibrosis (IPF), systemic scleroderma, non-alcoholic steatohepatitis and renal fibrosis. In IPF, increased levels of ATX are found in fibrotic lungs and high levels of LPA are observed in bronchoalveolar lavage fluid (BALF) exhaled breath condensate.[12-14] The involvement of LPA in IPF has been mostly linked to its effects on fibroblasts, promoting migration, proliferation and survival.[15-17] Earlier exploration of inhibition of ATX in IPF with ziritaxestat (GLPG1690) demonstrated efficacy in a mouse bleomycin-induced pulmonary fibrosis model.[15,16] In a clinical phase II study, ziritaxestat was shown to be well tolerated, while reducing plasma LPA C18:2 levels and stabilizing forced vital capacity after 12 weeks of treatment in IPF patients.[17] All development activities were discontinued, however, after observing an unfavorable benefit—risk profile when ziritaxestat was tested in combination with standard-of-care nintedanib and pirfenidone in clinical phase III studies (no data disclosed).

Shah et al.,[18] have previously reported the identification and optimization of a novel series of small molecule inhibitors of ATX, leading to the discovery of a compound with excellent enzyme potency and drug-like properties. Herein, we describe the preclinical and translational studies supporting the transition of IOA-289 (previously known as CRT0273750) into clinical development as a novel therapeutic approach for highly fibrotic tumor types that are resistant to current therapies.

MATERIALS AND METHODS

ATX activity assay

Pooled human plasma of mixed gender was obtained in a licensed laboratory (Poliklinika Bonifarm, Zagreb, Croatia) and incubated with IOA-289 (0.274-600 nM) at 37°C for 2 h. Plasma was analyzed for concentrations of LPA C16:0, LPA C18:1, LPA C18:2 and LPA C20:4 by liquid chromatography (LC)-mass spectrometry (MS)/MS. Male CD1 mice received a single 10 mg/kg oral dose of IOA-289 and terminal blood was collected at time points after dose (0.25-12 h). Control animals were sampled for baseline. Plasma was obtained and analyzed for concentrations of IOA-289 and pharmacokinetic biomarker LPA C18:2 by LC-MS/MS.

In vitro fibrosis panels

In vitro activity of IOA-289 on the modulation of biomarkers associated with fibrosis was characterized in the commercially available BioMAP Fibrosis phenotypic screening panel (Eurofins, St Charles, Missouri).[19] The BioMAP Fibrosis panel consists of systems that model fibrotic tissues and disease by co-culturing stimulated human primary cells: lung epithelial cells and fibroblasts; lung fibroblasts only; or renal epithelial cells with lung fibroblasts. The co-cultures are stimulated with transforming growth factor-β and tumor necrosis factor-α before incubation with IOA-289 (0.24-6 μM) for 48 h. Selected biomarkers are measured quantitatively by enzyme-linked immunosorbent assay (Supplementary Table S1, available at https://doi.org/10.1016/j.iotech.2023.100384).

Bleomycin lung fibrosis model

To induce fibrosis in the lungs, anesthetized male C57BL/6 mice were instilled intranasally with bleomycin at a concentration of 0.6 mg/ml or saline for the control group. Prophylactic treatment started at day 0 by administration of IOA-289 at 10 mg/kg or vehicle (methocel/phosphate-buffered saline) for treatment control groups by oral gavage. Treatment was carried out twice daily for 21 days, while monitoring body weight and overall condition of the animals. At day 21, mice were terminally bled to obtain plasma and lungs were excised. Plasma was analyzed by LC-MS/MS for levels of LPA C16:0, LPA C18:2, LPA C20:4 and LPA C22:4. Harvested lungs were fixed in 10% buffered formalin and paraffin embedded for histopathological evaluation. Tissue slides were stained according to Crossman's Trichrome and assessed using the Matsuse modification of Ashcroft score.[20,21] BALF was obtained at terminal procedure by two instillations of 0.5 ml ice cold saline via a cannula through the trachea and withdrawn with a syringe. BALF was collected in Protein LoBind tubes and centrifuged to obtain the supernatant for analysis of LPA C16:0, LPA C18:2, LPA C20:4 and LPA C22:4 levels by LC-MS/MS.

4T1 And E0771 tumor models

Female BALB/c mice were surgically implanted with 4T1 tumor cells in the mammary fat-pad and treatment with IOA-289 at 30 mg/kg twice a day (b.i.d.) by oral gavage started at day 7. Tumor growth was monitored twice weekly by three-dimensional caliper measurement. Tumors were harvested for immunohistochemistry and stained for presence of CD8+ T cells. To study metastasis, female BALB/c mice were surgically implanted with 4T1 tumor cells in the

mammary fat-pad and tumors were allowed to grow for 15 days. At day 15, primary tumors were resected, and mice were treated with IOA-289 at 100 mg/kg b.i.d. by oral gavage. At day 36, mice were killed and lungs were obtained for histological analysis and hind limbs were obtained for bone marrow collection to perform a colony formation assay. Bone marrow cells from flushed hind limbs were cultured for 14 days in complete media supplemented with 6-thioguanine (10 µg/ml) and the presence of colonies was visualized by crystal violet staining.

Female C57BL/6 mice were surgically implanted with E0771 tumor cells in the mammary fat-pad and treatment with IOA-289 at 30 mg/kg b.i.d. by oral gavage started at day 3 until termination at day 40. Tumor growth was monitored twice weekly by three-dimensional caliper measurement.

Non-clinical safety pharmacology and toxicology studies

A standard battery of non-clinical *in vitro* and *in vivo* safety pharmacology and toxicology studies have been conducted, including off-target profiling, G protein-coupled receptor (GPCR) profiling, receptor binding assays, human ether-a-go-go-related gene (hERG) assay, respiratory and neuro-cardiovascular *in vivo* studies, distribution and metabolism studies including drug interaction potential analyses. All studies were conducted as required by regulatory agencies and institutional guidelines and results are part of the submission documents required for clinical testing and not disclosed here.

Clinical healthy volunteer study

IOA-289 was tested in a first-in-human, randomized, double-blind, placebo-controlled, single ascending oral dose administration of IOA-289 to healthy male subjects in a fasted state. Five cohorts each of eight healthy subjects received single doses of escalating concentrations of IOA-289. For each cohort, subjects were randomized before dosing on day 1 to a single oral dose of IOA-289 or matching placebo capsules in a 6 : 2 ratio and dosed in two groups at least 48 h apart [two sentinel subjects (1 : 1) and six subjects (5 : 1), respectively]. Levels of IOA-289 and LPA C18:2 in circulation were analyzed by LC-MS/MS.[22] The IC_{50} value of IOA-289 on % LPA C18:2 reduction from baseline was calculated using a nonlinear regression fit analysis in GraphPad Prism.

RESULTS

IOA-289 is a selective and potent inhibitor of ATX

As described by Shah et al.,[18] IOA-289 (Figure 1A) is a potent ATX inhibitor binding to the LPC binding pocket of ATX and to the base of the LPA exit channel and hence is classified as a mixed type II/type IV inhibitor.[23] Pharmacodynamic activity of IOA-289 in human plasma was determined by measuring reduction in LPA C16:0, LPA C18:1, LPA C18:2 and LPA C20:4 as quantified by LC-MS/MS. After 2 h of incubation in human plasma, IOA-289 showed an average

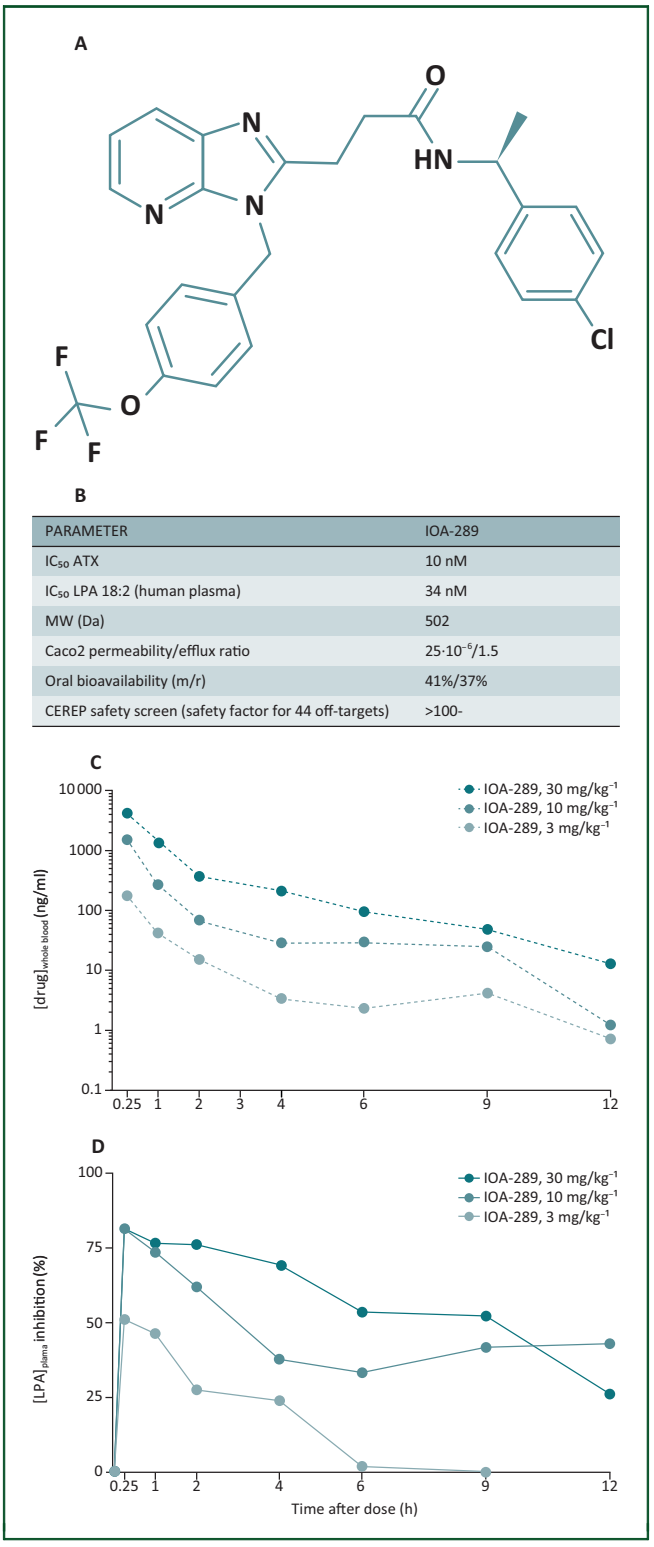

PARAMETER	IOA-289
IC_{50} ATX	10 nM
IC_{50} LPA 18:2 (human plasma)	34 nM
MW (Da)	502
Caco2 permeability/efflux ratio	$25 \cdot 10^{-6}$/1.5
Oral bioavailability (m/r)	41%/37%
CEREP safety screen (safety factor for 44 off-targets)	>100-

Figure 1. IOA-289 characteristics. The characteristics of IOA-289 show it is a selective and potent inhibitor of autotaxin activity. (A) IOA-289 chemical structure. (B) Summary of key features of IOA-289. (C) Male CD1 mice dosed with 3, 10 or 30 mg/kg of IOA-289 by oral gavage show clear exposure in plasma and (D) a dose-dependent reduction of circulating LPA C18:2 with an ED_{50} value at 1 h after dose of around 3 mg/kg.
LPA, lysophosphatidic acid.

IC_{50} of 36 nM (standard deviation = 5.5 nM) across all LPA species tested (Figure 1B). *In vivo* assessment of pharmacokinetic and pharmacodynamic activity of IOA-289 in male

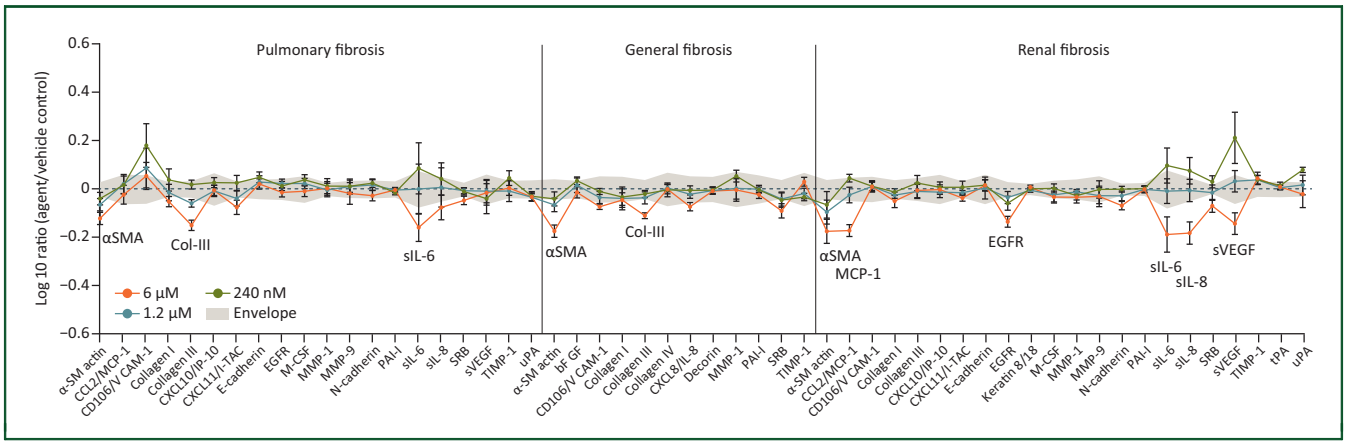

Figure 2. IOA-289 modulates fibrosis biomarkers *in vitro*. IOA-289 significantly modulates fibrosis biomarkers *in vitro* in the phenotypic screening panels that model fibrotic tissues and disease by co-culturing stimulated human primary cells; lung epithelial cells and fibroblasts, lung fibroblasts only or renal epithelial cells with lung fibroblasts. IOA-289 tested at concentrations of 6, 1.2 and 0.24 µM. At 6 µM (red line) IOA-289 decreased the activity of inflammation-related markers sIL-8, sIL-6 and MCP-1, the myofibroblast activation-related marker αSMA, the fibrosis-related matrix marker Col-III and the tissue remodeling/wound healing markers EGFR and sVEGF. The significance envelope (gray) represents the symmetrical upper and lower bound values of historical vehicle controls at a 95% confidence interval. Statistical analysis has been done by the service provider as described elsewhere.[19]
αSMA, α-smooth muscle actin; Col-III, collagen III; EGFR, epidermal growth factor receptor; MCP-1, monocyte chemoattractant protein 1; sIL, serum interleukin; sVEGF, soluble vascular endothelial growth factor.

CD1 mice at 3, 10 and 30 mg/kg by oral gavage showed a clear dose-proportional increase of plasma exposure of IOA-289 (Figure 1C) that correlated with a dose-dependent reduction of circulating LPA C18:2 with an ED_{50} value at 1 h after dose of around 3 mg/kg (Figure 1D).

IOA-289 is a potent modulator of fibrosis biomarkers

To characterize the effect of IOA-289 on human primary cells *in vitro*, fibrosis screening panels were used. These panels consist of three different cellular systems that model fibrotic tissue and disease states by co-culturing stimulated human primary cells: lung epithelial cells and fibroblasts, lung fibroblasts only or renal epithelial cells with lung fibroblasts. At a concentration of 6 µM, IOA-289 significantly decreased the activity of the inflammation-related markers soluble interleukin 8 and 6 (sIL-8, sIL-6) and monocyte chemoattractant protein *1* (MCP-1), the myofibroblast activation-related marker α-smooth muscle actin (αSMA), the fibrosis-related matrix marker collagen III (Col-III) and the tissue remodeling/wound healing markers epidermal growth factor receptor (EGFR) and soluble vascular endothelial growth factor (sVEGF) (Figure 2).

IOA-289 is efficacious in a model of lung fibrosis

To test the antifibrotic efficacy of IOA-289 in an established *in vivo* model for lung fibrosis, we deployed the bleomycin-induced pulmonary fibrosis (BLM) model in C57BL/6 mice with prophylactic IOA-289 treatment. In this model, inhibition of ATX has previously shown to be efficacious.[15,16] Histopathological evaluation of lung tissue after staining according to Crossman's Trichrome was assessed in a blinded manner using the modified Ashcroft score for fibrosis. IOA-289 showed significant reduction of collagen content and Ashcroft score, equal or better than standard-of-care nintedanib (Figure 3A and B). LPA C18:2 levels in plasma and BALF were significantly reduced by IOA-289 (Figure 3C and D). Of note, whereas the BLM model is known for its severity, which can be longitudinally followed by body weight measurements, treatment with IOA-289 alleviated the severity substantially compared with vehicle treatment (Supplementary Figure S1, available at https://doi.org/10.1016/j.iotech.2023.100384).

IOA-289 inhibits metastasis and tumor outgrowth in tumor models

Based on the demonstrated antifibrotic activity of IOA-289 in the BLM lung model, we hypothesized that IOA-289 should also be able to attenuate the growth of tumors *in vivo.* For this purpose, 4T1 tumors were orthotopically implanted in the mammary fat-pad of BALB/c mice to provide a fibrotic tumor and were treated with vehicle or IOA-289 starting on day 7 after tumor inoculation. In this immunocompetent tumor model, IOA-289 showed a statistically significant reduction of tumor outgrowth at day 22 as measured by AUC versus vehicle (Figure 4A and B). Flow cytometric analysis of the tumors obtained at day 22 showed higher infiltration of CD8+ T cells upon IOA-289 treatment compared with control (Figure 4C).

As ATX is also implicated in the motility and metastatic potential of tumor cells,[8] IOA-289 was tested for anti-metastatic potential. One day before inoculation of 4T1 cells in the mammary fat-pad, treatment with IOA-289 was started. Fifteen days after tumor inoculation, the primary tumors were surgically removed, and mice were taken off treatment (Figure 4D). In this short time frame, no effect was observed on primary tumor growth (Figure 4E). Twenty days after removal of the primary tumor, lungs and bone marrow cells from the mice were harvested (Figure 4D). Histological analysis of the lungs showed a marked reduction in metastatic burden for IOA-289-treated animals (Figure 4F). In addition, a colony formation assay from

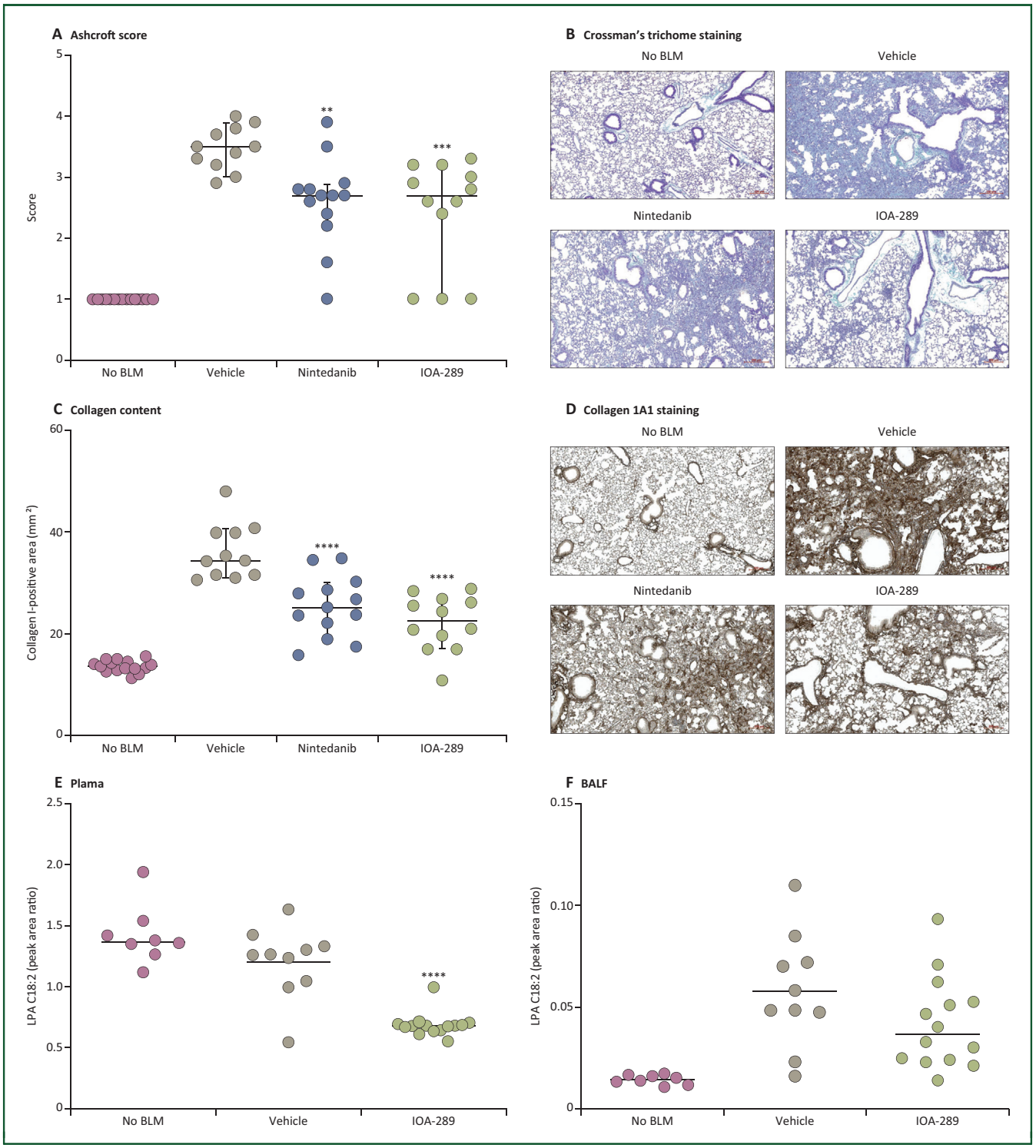

Figure 3. IOA-289 efficaciously reduces fibrosis *in vivo*. C57BL/6 mice were induced with bleomycin and treated with nintedanib, IOA-289 or vehicle for the duration of the experiment. Control mice were not induced with bleomycin (no BLM). Fibrosis levels as quantified per unbiased Ashcroft score (A), based on representative Crossman's Trichrome stainings (B). Fibrosis levels based on collagen content (C) upon quantification of collagen I stainings of lung tissue (D). LPA C18:2 levels in plasma (E); and BALF (F). Data were analyzed using Mann—Whitney test.
BALF, bronchoalveolar lavage fluid; LPA, lysophosphatidic acid.
**Indicates $P \leq 0.01$.
***Indicates $P \leq 0.001$.
****Indicates $P \leq 0.0001$.

cultured bone marrow showed marked reduction in bone metastases by IOA-289 (Figure 4G).

To further evaluate the *in vivo* therapeutic efficacy in breast cancer models, treatment with IOA-289 was also studied in the immunocompetent E0771 orthotopic mouse model. In this model, starting treatment with IOA-289 at day 3 reduced the tumor growth up until study termination at day 40 compared with the control group. In this model,

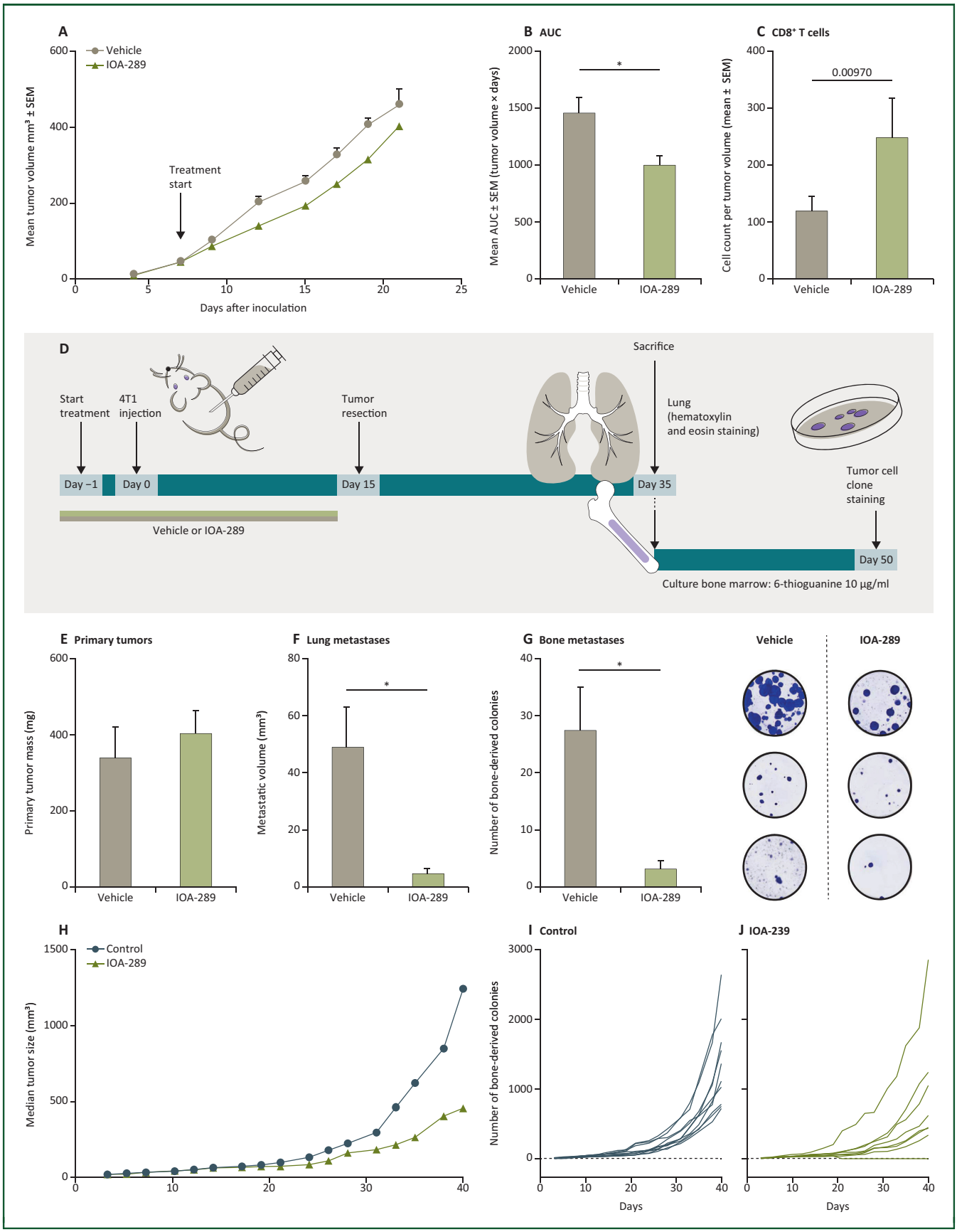

Figure 4. IOA-289 inhibits tumor outgrowth and metastasis. IOA-289 significantly reduces tumor outgrowth and metastasis in orthotopic mouse models of cancer. (A) Tumor growth and (B) mean AUC of 4T1 tumors orthotopically implanted and treated with vehicle or IOA-289; $n = 10$ mice per group. (C) Flow cytometric quantification of infiltrating CD8+ T cells in 4T1 tumors. (D) Schematic overview of the metastasis assays. IOA-289 or vehicle were administered for 15 days in mice orthotopically injected with 4T1 cells; $n = 12$ per group; (E) at day 15 the primary tumor was resected and weighted; at day 35 the mice were killed; (F) lungs were

IOA-289 inhibited tumor outgrowth and induced complete tumor eradication in two mice (Figure 4H-J). Taken together, these observations show that IOA-289 is able to strongly inhibit metastasis and the outgrowth of tumors in orthotopic mouse models at a range of doses.

Safety pharmacology and toxicology studies support further clinical development

IOA-289 was tested in a standard battery of non-clinical *in vitro* and *in vivo* [good laboratory practice (GLP)] safety pharmacology and toxicology studies (results not shown). *In vitro* safety pharmacology studies showed that IOA-289 has no to minimal potential off-target interactions: on a panel of lipid receptors (LPA1, LPA2, LPA3, LPA5, S1P1, S1P2, SP3, S1P4 and S1P5) and on the SafetyScreen44™ panel, IOA-289 only showed sub-micromolar binding to the 5-hydroxytryptamine 2B (5-HT2B) receptor and was confirmed to be an antagonist of 5-HT2B with an IC_{50} value of 2.5 μM. In the GLP hERG assay, IOA-289 inhibited the hERG tail current with an IC_{50} of 1.03 μM. Based on the high potency of IOA-289 in human plasma and the relatively high plasma protein binding in human of 99%, these activities are not considered to be a significant safety concern and do not impede further development.

In vivo GLP safety pharmacology studies showed that IOA-289 has no relevant effects on respiratory functions in rats and cardiovascular (including QTc changes) and neurobehavioral functions in dogs. Toxicology testing in the 4-week GLP studies in rats and dogs gave oral no observed adverse effect levels (NOAELs) of 300 mg/kg/day and 60 mg/kg/day for IOA-289, respectively. The main target organs for toxicity for IOA-289 in rats were the liver, the bone marrow and the stomach in both sexes and additionally the kidneys, the testes and thyroids in males. All findings were reversible, however, and after the recovery period the testes revealed normal progression of the spermatogenic cycle. The main target organs for toxicity for IOA-289 in dogs were the gastrointestinal tract, the liver, the bladder and the parotid gland. Based on the absence of *in vitro* toxicology findings, IOA-289 is considered to carry a low risk for genotoxicity, phototoxicity and cytotoxicity. These safety pharmacology and toxicology studies supported progression into clinical trials.

Randomized, double-blind, placebo-controlled study of single ascending oral doses of IOA-289

IOA-289 was tested in a first-in-human clinical phase I study in healthy male volunteers (NCT05027568). This healthy volunteer study was designed to test the safety and tolerability of escalating doses of IOA-289 following a single oral dose administration and was completed without any protocol deviations. Also, the pharmacokinetic and pharmacodynamic parameters by reduction of LPA C18:2 were investigated. IOA-289 was well tolerated and no clinically significant treatment- or dose-related trends in vital signs, clinical laboratory evaluations, physical examination and 12-lead ECGs were observed. Plasma exposure was measured up to 24 h after dose. Maximum concentrations were measured 1 h after dose administration and increased dose proportionally (Figure 5A) and IOA 289 produced a dose-related decrease in circulating levels of LPA C18:2, with maximal inhibition of LPA C18:2 observed at the cohorts 4 and 5 dose levels (Figure 5B). Inhibition of LPA C18:2 peaked at 1-2 h after dose and gradually decreased thereafter. When pharmacokinetic data were directly correlated to pharmacodynamic data, the resulting IC_{50} value of IOA-289 on % LPA C18:2 reduction from baseline was calculated as 15 ng/ml in human plasma (Figure 5C).

DISCUSSION

Despite the advances in the treatment of cancer in the last few decades, a large proportion of tumors remain resistant to conventional treatments such as chemotherapy and radiotherapy. Durable responses to immunotherapy are only seen in a minority of patients, and all these therapies come with an increased risk of severe toxicities.[24] Therefore, there is still a large unmet need for new avenues of research into novel pathways and targets that can overcome these resistance mechanisms. Increasing evidence points to the role of the tumor stroma in nourishing cancer growth and maintaining treatment resistance.[7] As the ATX-LPA pathway has been implicated in tumor growth, metastasis and the interface of the tumor with the stromal and immune microenvironment, we set out to test the hypothesis that inhibition of ATX could represent a novel treatment strategy for cancer.

IOA-289 (CRT0273750) was discovered from a novel series of ATX inhibitors based on the imidazopyridine scaffold.[18] Structural studies have established that ATX has a tripartite binding site, consisting of the catalytic zinc site, a hydrophobic pocket that acts as the LPC substrate docking site and a tunnel that acts as a protective carrier site for the highly labile product of ATX activity, LPA.[1,25] Several inhibitors of the enzyme ATX have previously been described and these have been classified by their structural binding mode into four types, type I-IV.[23,26] IOA-289 is shown to bind to the LPC substrate channel as well as partially blocking the base of the tunnel, designating it as a mixed type II/type IV inhibitor based on this classification, and placing it in an inhibitor class of its own. Avoidance of interaction with the enzymatic site likely contributes to the improved safety profile of IOA-289 compared with other

fixed and stained with H&E to allow detection of metastasis; (G) bones were collected and bone marrow isolated and grown in culture in presence of 6-thioguanine 10 μ/ml; at day 50 colonies were stained with crystal violet; quantification and representative pictures of the colonies from three mice are shown. Orthotopic E0771 breast cancer model treated with vehicle or IOA-289. Median tumor growths (H) and individual growth of vehicle (I) and IOA-289 (J) are shown; $n = 10$ per group. All graphs show mean or median ± SEM. Unpaired *t*-test was used to test significance.
H&E, hematoxylin—eosin; SEM, standard error of the mean.
**Indicates $P \leq 0.01$.

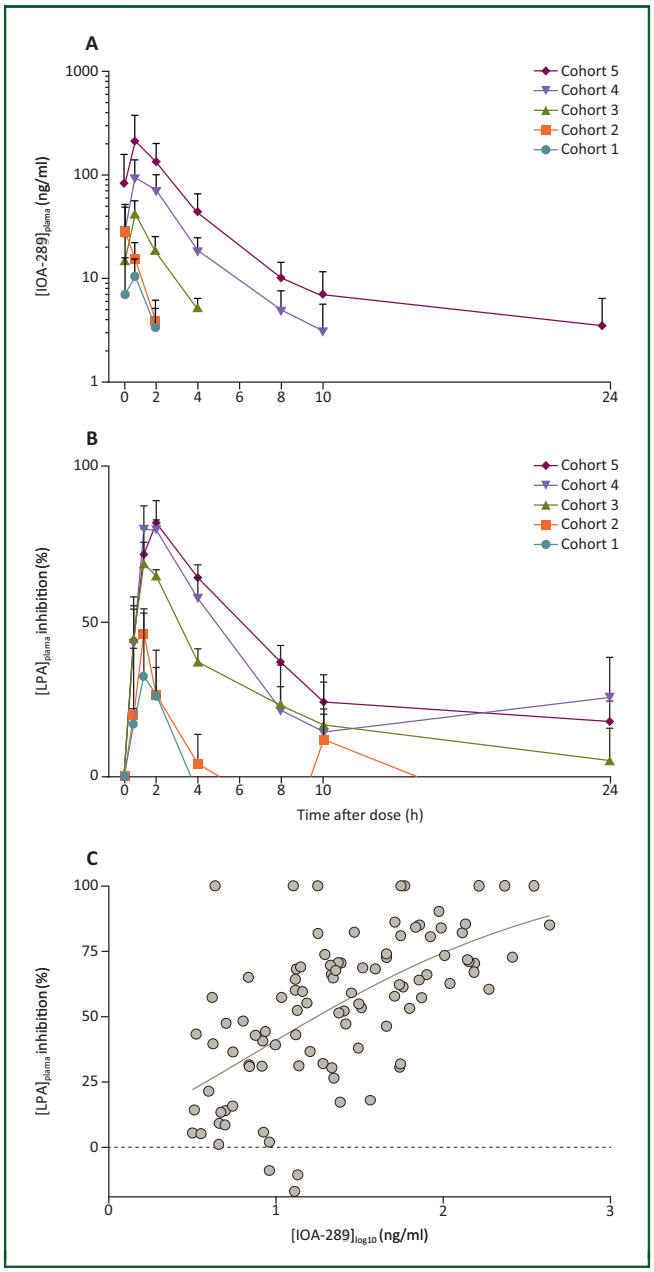

Figure 5. Randomized, double-blind, placebo-controlled study of single ascending oral doses of IOA-289. Healthy male volunteers were administered a single dose of IOA-289 in a capsule formulation (six active subjects per cohort, placebo not analyzed), at increasing dose levels. Plasma exposure of IOA-289 was measured up to 24 h after dose (A). LPA C18:2 in plasma was measured at baseline and up to 24 h after dose; data are % inhibition of baseline levels (B). Using the pharmacokinetic and pharmacodynamic data, the IC_{50} of IOA-289 was calculated as 15 ng/ml in human plasma (C).
LPA, lysophosphatidic acid.

ATX inhibitors, as this avoids off-target toxicities that were seen with first-generation entities.[26,27]

ATX was first isolated from the culture media of melanoma cells, and was shown to be an autocrine motility-stimulating factor.[28] Subsequently, ATX was identified as the plasma lysoPLD factor responsible for the generation of the majority of extracellular LPA.[29,30] Due to the central role for LPA in wound healing, therapeutic strategies targeting either the generation of LPA via ATX inhibition, or antagonists of LPA receptors (LPARs) became the focus of efforts to develop novel therapies for organ-specific fibrosis such as IPF. We show that IOA-289 modulates biomarkers of fibrosis *in vitro*, with notable effects on α-SMA and collagen III. This activity translates into *in vivo* efficacy as demonstrated by the highly significant reduction of lung fibrosis and corresponding reduction in lung collagen deposition by IOA-289 in the widely accepted mouse model of lung fibrosis, the bleomycin-induced lung injury model. Furthermore, we showed that the product of ATX activity, LPA, can be measured as both a circulating and tissue-specific biomarker of ATX inhibition by IOA-289.

As ATX was initially identified as a secreted factor from melanoma cells, subsequent studies have shown that ATX knock down as well as pharmacological inhibition of ATX attenuate metastasis in mouse models of cancer.[31] The studies that formed the basis of these observations, however, were conducted in xenograft models, i.e. in the absence of a full immune system, and therefore certain aspects of ATX inhibition in the tumor stroma that could contribute to anticancer mechanisms were initially overlooked. T cells have been shown to express LPARs and recently Matas-Rico et al.,[11] demonstrated that LPA is chemorepulsive for T cells and IOA-289 can rescue tumor-infiltrating lymphocyte (TIL) migration *in vitro*. This, together with the translational observation that there is an inverse correlation between intratumoral ENPP2 expression and CD8+ T cell accumulation in melanoma tumors[11] suggests that ATX inhibition could play a role in inhibiting cancer growth and survival through disrupting the tumor-stroma-immune interface. In the 4T1 model we showed that whilst treatment with IOA-289 had no effect on the primary tumor growth, there was a strong reduction in metastases to both the lung and the bone. These data are in agreement with other studies showing the ability of ATX to promote lung metastasis in preclinical models of melanoma[32] and ras-transformed NIH3T3 fibroblasts.[33]

The 4T1 tumor model is considered immunologically 'cold', with limited T-cell infiltration and generally resistant to checkpoint blockade.[34] Flow cytometric assessment of lymphocytes isolated from 4T1 tumors revealed a trend in increased numbers of CD8+ T cells infiltrating into the primary tumors. Even though we did not explore the molecular mechanism behind this observation, it is possible that, as it occurs in melanoma, LPAR6 expression in TILs act as a repulsion signal in this ATX-enriched breast tumor.[11] Interestingly, LPA has been shown to impair CD8+ T-cell activation through binding LPAR5 and disrupting early T-cell receptor (TCR) activation.[33] Whether the CD8+ T cells infiltrating the tumor microenvironment in the IOA-289-treated group are also more cytotoxic needs to be further investigated.

In addition to the antimetastatic effect observed in the 4T1 tumor model, IOA-289 suppressed the growth of E0771 primary breast tumors, with two complete responses. Further work is needed to understand the differences between the tumor and microenvironmental status of these two models to account for the difference in effects of ATX

inhibition by IOA-289. These data, however, confirm the role for ATX in the promotion of both primary and metastatic cancer processes and further support the finding that the ATX-LPA pathway can drive a reduction in T-cell infiltration into tumors that can be overcome by pharmacological intervention, suggesting that ATX inhibition can at least in part switch a tumor from a cold to a hot phenotype.

In preliminary mouse studies, we showed that IOA-289 was bioavailable following oral dosing, and that exposure in the plasma corresponded with a dose-proportional reduction in circulating LPA. In non-clinical (GLP) safety pharmacology and toxicology studies, IOA-289 proved to be safe and well tolerated in both rats and dogs, thus enabling the testing of IOA-289 in the human setting. In a first-in-human, phase I study (NCT05027568), IOA-289 was well tolerated with no adverse events reported. Measured exposure was dose proportional for C_{max}, and the IC_{50} inhibition of circulating LPA was calculated at 15 ng/ml which corresponds with the measured inhibition of LPA in the human plasma *in vitro* assay.

Based on these and other unpublished preclinical data, a clinical study evaluating IOA-289 in combination with standard-of-care chemotherapy in pancreatic cancer patients has recently been initiated (NCT05586516).

ACKNOWLEDGEMENTS

We would like to thank all collaborators and CROs who were involved in the studies, this includes Fidelta (Croatia, now Selvita) for the ATX/LPA assays and lung fibrosis model, Aptuit (Italy, now Evotec) for the non-clinical safety studies and clinical bioanalysis, Eurofins (USA) for the BioMAP Fibrosis assay, CrownBio (UK) and KWS BioTest (UK, now Charles River) for the 4T1 tumor models and MI Bioresearch (USA, now Labcorp Drug Development Inc.) for the E0771 tumor model. We also thank Centro Ricerche Cliniche di Verona (Italy) for executing the clinical study and the healthy volunteers for participating.

FUNDING

This work was supported by iOnctura (no grant number).

DISCLOSURE

MAD, KNS, CP, ML, LV and ZJ are employed by and shareholders of iOnctura. All other authors are employed by institutions or companies that have been financially compensated by iOnctura to conduct the discussed research. All research has been carried out to high scientific standards and integrity and according to applicable regulatory guidelines.

REFERENCES

1. Perrakis A, Moolenaar WH. Autotaxin: structure-function and signaling. *J Lipid Res*. 2014;55:1010-1018.
2. Geraldo LHM, Spohr TCLS, Amaral RFD, et al. Role of lysophosphatidic acid and its receptors in health and disease: novel therapeutic strategies. *Signal Transduct Target Ther*. 2021;6:45.
3. Moolenaar WH. Development of our current understanding of bioactive lysophospholipids. *Ann N Y Acad Sci*. 2000;905:1-10.
4. Balazs L, Okolicany J, Ferrebee M, Tolley B, Tigyi G. Topical application of the phospholipid growth factor lysophosphatidic acid promotes wound healing in vivo. *Am J Physiol Regul Integr Comp Physiol*. 2001;280:R466-R472.
5. Hemmings DG, Brindley DN. Signalling by lysophosphatidate and its health implications. *Essays Biochem*. 2020;64(3):547-563.
6. Willier S, Butt E, Grunewald TGP. Lysophosphatidic acid (LPA) signalling in cell migration and cancer invasion: a focussed review and analysis of LPA receptor gene expression on the basis of more than 1700 cancer microarrays. *Biol Cell*. 2013;105:317-333.
7. Bagaev A, Kotlov N, Nomie K, et al. Conserved pan-cancer microenvironment subtypes predict response to immunotherapy. *Cancer Cell*. 2021;39:845-865.e7.
8. Auciello FR, Bulusu V, Oon C, et al. A stromal lysolipid-autotaxin signaling axis promotes pancreatic tumor progression. *Cancer Discov*. 2019;9:617-627.
9. Benesch MG, Tang X, Maeda T, et al. Inhibition of autotaxin delays breast tumor growth and lung metastasis in mice. *FASEB J*. 2014;28:2655-2666.
10. Oda SK, Strauch P, Fujiwara Y, et al. Lysophosphatidic acid inhibits CD8 T-cell activation and control of tumor progression. *Cancer Immunol Res*. 2013;1:245-255.
11. Matas-Rico E, Frijlink E, van der Haar Àvila I, et al. Autotaxin impedes anti-tumor immunity by suppressing chemotaxis and tumor infiltration of CD8+ T cells. *Cell Rep*. 2021;37:110013.
12. Oikonomou N, Mouratis MA, Tzouvelekis A, et al. Pulmonary autotaxin expression contributes to the pathogenesis of pulmonary fibrosis. *Am J Respir Cell Mol Biol*. 2012;47:566-574.
13. Montesi SB, Mathai SK, Brenner LN, et al. Docosatetraenoyl LPA is elevated in exhaled breath condensate in idiopathic pulmonary fibrosis. *BMC Pulm Med*. 2014;14:5.
14. Ninou I, Sevastou I, Magkrioti C, et al. Genetic deletion of autotaxin from CD11b+ cells decreases the severity of experimental autoimmune encephalomyelitis. *PLoS One*. 2020;15:e0226050.
15. Desroy N, Housseman C, Bock X, et al. Discovery of 2-[[2-ethyl-6-[4-[2-(3-hydroxyazetidin-1-yl)-2-oxo-ethyl]piperazin-1-yl]-8-methyl-imidazo[1,2-a]pyridin-3-yl]-methyl-amino]-4-(4-fluorophenyl)thiazole-5-carbonitrile (GLPG1690), a first-in-class autotaxin inhibitor undergoing clinical evaluation for the treatment of idiopathic pulmonary fibrosis. *J Med Chem*. 2017;60(9):3580-3590.
16. Murgo A, Canciani B, Fragni D, et al. The Autotaxin Inhibitor GLPG1690 Attenuates Bleomycin-Induced Pulmonary Fibrosis in Mice. A5239. https://doi.org/10.1164/ajrccm-conference.2019.199.1_MeetingAbstracts.A5239. Accessed May 21, 2019.
17. Maher TM, van der Aar EM, Van de Steen O, et al. Safety, tolerability, pharmacokinetics, and pharmacodynamics of GLPG1690, a novel autotaxin inhibitor, to treat idiopathic pulmonary fibrosis (FLORA): a phase 2a randomised placebo-controlled trial. *Lancet Respir Med*. 2018;6(8):627-635.
18. Shah P, Cheasty A, Foxton C, et al. Discovery of potent inhibitors of the lysophospholipase autotaxin. *Bioorg Med Chem Lett*. 2016;26:5403-5410.
19. Shah F, Stepan AF, O'Mahony A, et al. Mechanisms of skin toxicity associated with metabotropic glutamate receptor 5 negative allosteric modulators. *Cell Chem Biol*. 2017;24:858-869.e5.
20. Ashcroft T, Simpson JM, Timbrell V. Simple method of estimating severity of pulmonary fibrosis on a numerical scale. *J Clin Pathol*. 1988;41:467-470.
21. Matsuse T, Teramoto S, Katayama H, et al. ICAM-1 mediates lung leukocyte recruitment but not pulmonary fibrosis in a murine model of bleomycin-induced lung injury. *Eur Respir J*. 1999;13:78-81.
22. Mameli M, Franchi J, Calusi G, et al. Validation of an LC—MS/MS method for the quantification IOA-289 in human plasma and its application in a first-in-human clinical trial. *J Pharm Biomed Anal*. 2022;217:114829.
23. Salgado-Polo F, Perrakis A. The structural binding mode of the four autotaxin inhibitor types that differentially affect catalytic and non-catalytic functions. *Cancers*. 2019;11:1577.

24. Wolchok JD, Hoos A, O'Day S, et al. Guidelines for the evaluation of immune therapy activity in solid tumors: immune-related response criteria. *Clin Cancer Res*. 2009;15:7412-7420.
25. Hausmann J, Kamtekar S, Christodoulou E, et al. Structural basis of substrate discrimination and integrin binding by autotaxin. *Nat Struct Mol Biol*. 2011;18:198-204.
26. Thomson CG, Le Grand D, Dowling M, et al. Development of autotaxin inhibitors: a series of zinc binding triazoles. *Bioorg Med Chem Lett*. 2018;28:2279-2284.
27. van Meeteren LA, Ruurs P, Stortelers C, et al. Autotaxin, a secreted lysophospholipase D, is essential for blood vessel formation during development. *Mol Cell Biol*. 2006;26:5015-5022.
28. Stracke ML, Krutzsch HC, Unsworth EJ, et al. Identification, purification, and partial sequence analysis of autotaxin, a novel motility-stimulating protein. *J Biol Chem*. 1992;267:2524-2529.
29. Tokumura A. Physiological and pathophysiological roles of lysophosphatidic acids produced by secretory lysophospholipase D in body fluids. *Biochim Biophys Acta*. 2002;1582:18-25.
30. Umezu-Goto M, Kishi Y, Taira A, et al. Autotaxin has lysophospholipase D activity leading to tumor cell growth and motility by lysophosphatidic acid production. *J Cell Biology*. 2002;158:227-233.
31. Leblanc R, Lee SC, David M, et al. Interaction of platelet-derived autotaxin with tumor integrin $\alpha V\beta 3$ controls metastasis of breast cancer cells to bone. *Blood*. 2014;124:3141-3150.
32. Dacheux MA, Lee SC, Shin Y, et al. Prometastatic effect of ATX derived from alveolar type II pneumocytes and B16-F10 melanoma cells. *Cancers*. 2022;14:1586.
33. Mathew D, Kremer KN, Strauch P, Tigyi G, Pelanda R, Torres RM. LPA5 is an inhibitory receptor that suppresses CD8 T-cell cytotoxic function via disruption of early TCR signaling. *Front Immunol*. 2019;10:1159.
34. Fabian KP, Padget MR, Fujii R, Schlom J, Hodge JW. Differential combination immunotherapy requirements for inflamed (warm) tumors versus T cell excluded (cool) tumors: engage, expand, enable, and evolve. *J Immunother Cancer*. 2021;9:e001691.